

Supplementary material

Fabrication of ionogels

The ionogels are synthesized by free radical polymerization of acrylic acid (AA) and acrylamide (AAM) in the ionic liquid 1-ethyl-3-methylimidazolium ethylsulfate ($[\text{C}_2\text{min}][\text{EtSO}_4]$) (Fig. S1). In the ionic liquid, we dissolve AA at 4.8 mol/L and AAM at 1.2 mol/L as the monomers of the polymer network, poly(ethylene glycol) diacrylate (PEGDA) at 0.036 mol/L as the cross-linker, and α -ketoglutaric acid at 0.006 mol/L as the initiator. Then, the solution is transferred into a mold made of a pair of glass plates separated by a silicone spacer. To make the ionogel easily removed from the mold without damaging the surface, the glass plates are treated with Trichloro (1H, 1H, 2H, 2H-perfluorooctyl) silane (TPFS) using chemical vapor deposition method.¹ Polymerization is carried out under ultraviolet light with a power of 50 W and a wavelength of 365 nm for 1 h. We control the thickness of the ionogel by adjusting the thickness of the silicone spacer.

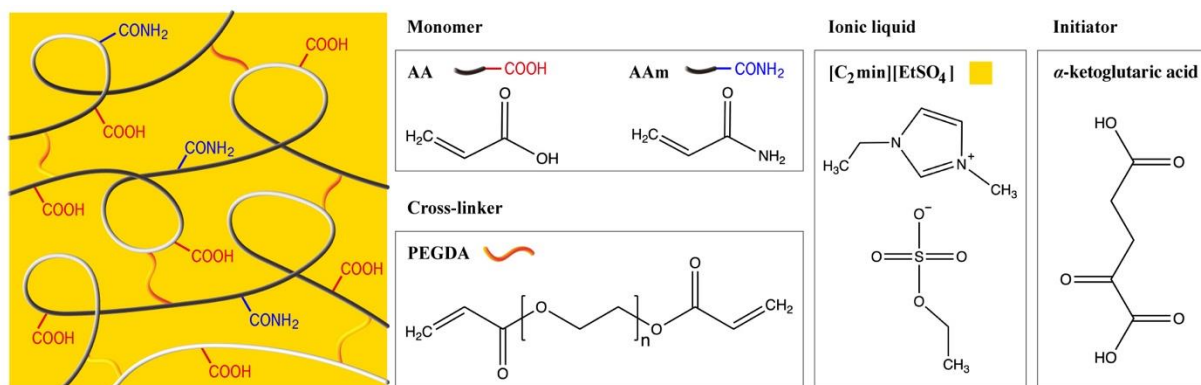


Figure S1. Fabrication of Poly(acrylamide-*co*-acrylic acid) ionogel. Ingredients: acrylic acid (AA) and acrylamide (AAM) as the monomers of the polymer network, poly(ethylene glycol) diacrylate (PEGDA) as the cross-linker, 1-ethyl-3-methylimidazolium ethyl sulfate ($[\text{C}_2\text{mim}][\text{EtSO}_4]$) as the ionic liquid, and α -ketoglutaric acid as the initiator.

Swelling ratio of the ionogel

The swelling ratio of the ionogel is computed from

$$J = 1 + \frac{(m_{\text{gel}} - m_{\text{dry}})/\rho_{[\text{C}_2\text{min}][\text{EtSO}_4]}}{m_{\text{dry}}/\rho_{\text{PAA-co-AAM}}} \quad (\text{S1})$$

Here the density of the ionic liquid at 60 °C is $\rho_{[\text{C}_2\text{min}][\text{EtSO}_4]} = 1.21484 \text{ g/cm}^3$.² The density of polyacrylamide is $\rho_{\text{PAAM}} = 1.443 \text{ g/cm}^3$,³ and the density of poly(acrylic acid) is $\rho_{\text{PAA}} = 1.41 \text{ g/cm}^3$,⁴ thus the density of the poly(acrylamide-*co*-acrylic acid) is $\rho_{\text{PAA-co-AA}} = (\rho_{\text{PAAM}} + 4\rho_{\text{PAA}})/5 = 1.42 \text{ g/cm}^3$. The mass of the swollen ionogel m_{gel} is measured directly, while the mass of the dry network m_{dry} is calculated from the recipe in synthesis. Here we assume that all monomers are completely reacted.

Inhabiting the hygroscopicity of ionic liquid

To prevent the ionogel from absorbing humidity from the ambient, all measurements are conducted at an elevated temperature of 60 °C. We have heated the ionic liquid ($[\text{C}_2\text{min}][\text{EtSO}_4]$) to this temperature and tracked its weight change. The weight of the ionic liquid increases by less than 0.2% within 120 h, proving that the hygroscopicity can be neglected at this temperature, Fig. S2.

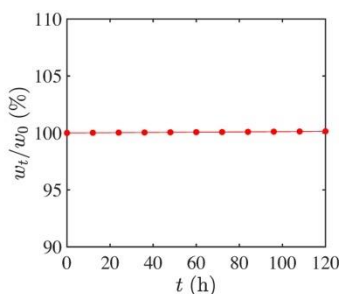


Figure S2. Weight change of the ionic liquid at 60 °C.

Measurement of shear modulus and osmotic pressure

We use a mechanical testing machine (INSTRON 5966) to measure the shear modulus and osmotic pressure of the as-synthesized and swollen ionogels. To measure the shear modulus of the as-synthesized and swollen ionogels, we synthesize an ionogel sheet with $1\ \mu\text{m}$ thickness. After swelling to the desired swelling ratio, we cut the ionogel sheet into disks of 10 mm in diameter. A compression test is then performed to measure the shear modulus (Fig. S3a). The stress-strain curve recorded by the machine is fitted with the neo-Hookean model to calculate the shear modulus. While for the measurement of osmotic pressure, we synthesize a thinner ionogel sheet with $0.3\ \mu\text{m}$ thickness. The as-synthesized and swollen ionogels are cut into disks of 15 mm in diameter, and their osmotic pressure is measured with a constrained swelling test (Fig. S3b). Here the gel disk is glued to an acrylic sheet to constrain the lateral swelling. The disk is placed on filter paper inside a petri dish filled with the ionic liquid. The filter paper ensures that the ionogel is in contact with the ionic liquid over the entire bottom surface. At equilibrium, the force measured by the load cell to constrain the swelling equals the osmotic pressure Π . During these tests, a feedback-controlled heater is used to maintain a temperature of $60\ ^\circ\text{C}$.

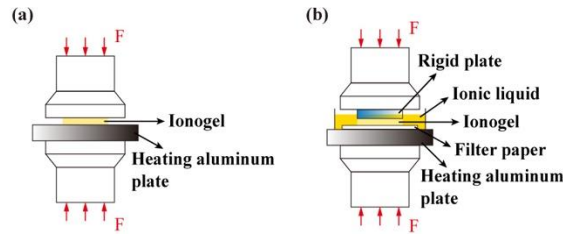


Figure S3. Schematic illustration of the measurement setup for the (a) Shear modulus, and (b) Osmotic pressure.

Surface topography measurement

We utilize a white light interferometer (Zeta-20) to scan the surface topography of the as-synthesized and swollen ionogels, which is rapid and non-contact. Through stitching 9×12 measurements (Fig. S4a), we obtain the topography of a surface with a size 11520×11520 pixels and a resolution $0.258\ \mu\text{m}$. We have scanned the topography of the sandblasted glass over two different regions, Fig. S4b. We find that the two PSDs differ in long wavelengths greater than $60\ \mu\text{m}$ but coincide in shorter wavelengths, which suggests that the long wavelength features are not sufficiently averaged in the PSD and the statistical property of the shorter wavelength features are independent of regions. On the other hand, when comparing the PSDs from samples of different swelling ratios, all the PSDs deviate from the trend at the longer wavelength when the feature size is smaller than $2\ \mu\text{m}$ and approach an identical limit, Fig. S4c. This short wavelength behavior is likely caused by the diffraction limit of the white light interferometry, which leads to the inaccurate measurement for features $\sim 1\ \mu\text{m}$ or smaller. To avoid these artifacts, we limit our theoretical analysis to features in the range of $2 - 60\ \mu\text{m}$, which covers the length scales we need to investigate the elastocapillary and osmocapillary effects on ionogels' surface topography.

To compare the PSD of the as-synthesized ionogel surface and the sandblasted glass, we plot their ratio in a log-log plot (Fig. S4c). This ratio is close to 1 and oscillates in a small range, proving that there are some damages to the as-synthesized ionogel surface due to peeling the surface off the glass mold, but these damages are negligible in the analysis region of $2 - 60\ \mu\text{m}$.

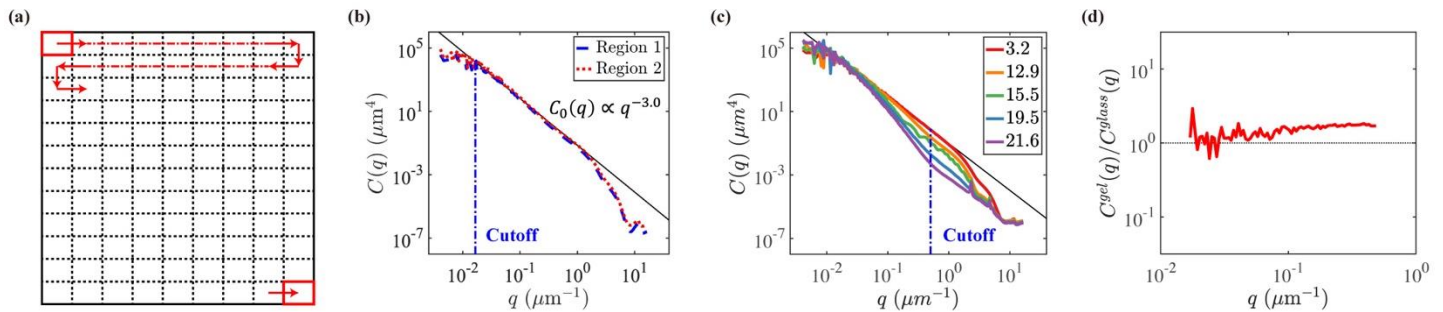


Figure S4. Surface topography measurement. (a) Expanding the measurement area through the stitching method. After the white light interferometer scans an area, it will move to the next adjacent area until all the set areas are scanned. Then we stitch all the measurements of different areas to obtain the surface topology of the whole area. (b) Full range PSD of measured topography for sandblasted glass in two different regions. The cutoff of the PSD in the long wavelength is $60\ \mu\text{m}$. (c) Full range PSD of measured topography for each sample. The cutoff of the PSD in the short wavelength is $2\ \mu\text{m}$. (d) The ratio between the PSD of the as-synthesized ionogel surface and the averaged PSD of the sandblasted glass. This ratio is close to 1, indicating that the damages to the as-synthesized ionogel surface are negligible.

The effect of isotropic swelling on PSD

Consider the isotropic swelling with a swelling ratio $J = V/V_{net}$, where V and V_{net} are the volume of the gel and the volume of the dry polymer network. Denote J_0 as the swelling ratio of the as-synthesized ionogel. Then a point on the gel surface with the coordinate (x_1, x_2) will be moved to $(x'_1, x'_2) = ((J/J_0)^{1/3}x_1, (J/J_0)^{1/3}x_2)$ after swelling, Figure S5a. The stress-free surface profile height $h_0(x_1, x_2)$ will be transformed to $h'_0(x'_1, x'_2) = (J/J_0)^{1/3}h_0(x_1, x_2)$. In the Fourier space, the wavevector (q_1, q_2) will be transformed to $(q'_1, q'_2) = ((J/J_0)^{-1/3}q_1, (J/J_0)^{-1/3}q_2)$ while the Fourier transform of $h_0(x_1, x_2)$, $\tilde{h}_0(q_1, q_2)$, will be transformed to

$$\begin{aligned}\tilde{h}'_0(q'_1, q'_2) &= \iint h_0(x'_1, x'_2) e^{-i(q'_1 x'_1 + q'_2 x'_2)} dx'_1 dx'_2 \\ &= (J/J_0) \iint h_0(x_1, x_2) e^{-i(q_1 x_1 + q_2 x_2)} dx_1 dx_2 = (J/J_0) \tilde{h}_0(q_1, q_2)\end{aligned}\quad (\text{S2})$$

Recall the definition of PSD in Eq. 1, since $A'_0 = (J/J_0)^{2/3}A_0$, then $C'_0 = |\tilde{h}'_0|^2 / (4\pi^2 A'_0) = (J/J_0)^{4/3}C_0$. Therefore, the isotropically swollen PSD can be obtained by transforming the as-synthesized PSD by $q' = q(J/J_0)^{-1/3}$ and $C'_0 = C_0(J/J_0)^{4/3}$, Fig. S5b.

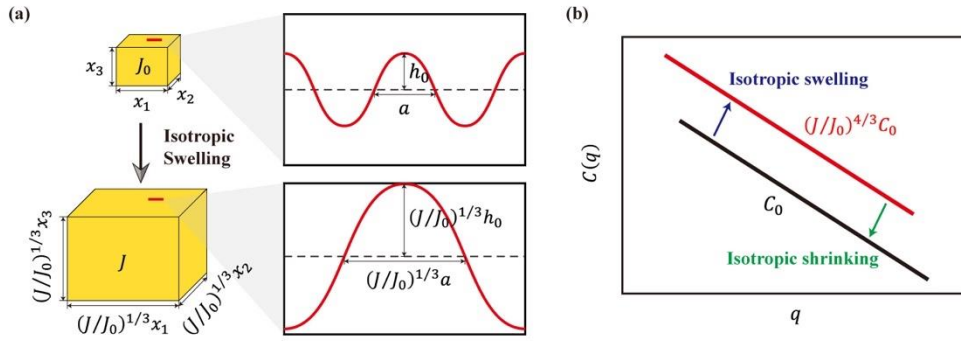


Figure S5. The effect of isotropic swelling on surface topography. (a) Schematic of isotropic swelling. (b) The effect of isotropic swelling on PSD.

Simulation parameters for each sample

Table S1. Simulation parameters for as-synthesized and swollen ionogel samples. The deviation Dev^{elasto} is computed based on linear elastocapillary model with the measured shear modulus shown in Fig. 2a.

Name	Swelling ratio J	μ (kPa)	Poisson's ratio	Dev^{elasto} (%)	Π (kPa)	Dev^{osmo} (%)
Sample 1	3.2	42.95	0.35	0.19	/	/
Sample 2	12.9	17.08	0.35	0.36	/	/
Sample 3	15.5	7.30	0.35	1.58	1.82	0.87
Sample 4	19.5	4.47	0.35	3.78	0.82	0.39
Sample 5	21.6	4.74	0.35	11.85	0.41	0.33

Comparison between experimental and predictive PSD

To highlight the difference between the prediction and experiment, we also plot the ratio between $C(q)$ and $C_0(q)$:

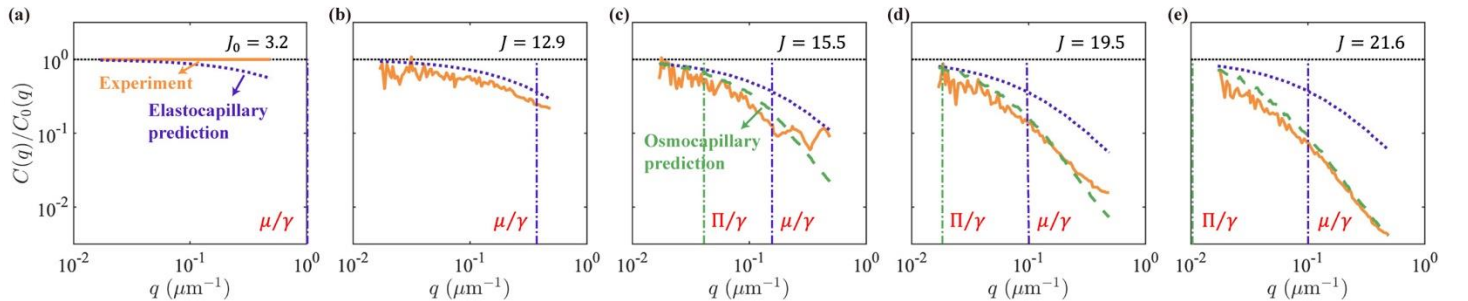


Figure S6. Comparison between experimental and predictive PSD for samples of swelling ratio (a) $J_0 = 3.2$, (b) $J = 12.9$, (c) $J = 15.5$, (d) $J = 19.5$, and (e) $J = 21.6$.

The effect of Π/μ on the osmcapillary PSD prediction

To investigate the effect of Π/μ on the osmcapillary PSD prediction, we conduct simulations on a random isotropic self-affine rough surface, which is artificially generated by the authors.⁵ This surface has a PSD of $C_0(q) = Dq^{-2(H+1)}$ and a size of $2^{14} \times 2^{14}$ pixels. Since only one of γ/μ and γ/Π governs the gel surface behavior, we set the dominant capillary length $l_c = \max\{\gamma/\mu, \gamma/\Pi\} = 60$ pixels and vary Π/μ from 10^{-3} to 10^3 . We plot the dimensionless osmcapillary PSD in Fig. S7a. Here the PSD is normalized by D^{-1} and $(l_c)^{-2(H+1)}$, and q is normalized by l_c . It shows that all the dimensionless osmcapillary PSD start to deviate obviously from the stress-free PSD around $ql_c = 10^0$. In addition, the dimensionless osmcapillary PSD for $\Pi/\mu = 10^1$ and $\Pi/\mu = 10^2$ overlaps with each other, showing that the elastocapillary limitation has been achieved when $\Pi/\mu = 10^1$. To further observe the deviation of the dimensionless osmcapillary PSD, we take their derivatives in log-log plot and subtract them with the power law of stress-free PSD, which allows us to track the change in power law with ql_c (Fig. S7b). Their change in power law increases as ql_c increases and reaches a relatively large value around $ql_c = 10^0$, which confirms our observation in Fig. S7a. In addition, their change in power law reaches a plateau value as ql_c continues to increase, which evaluates the extent of deviation and is termed as the equilibrium change in power law, Δn . When ql_c gradually approaches the maximum, the change in power law fluctuates due to the finite size effect.

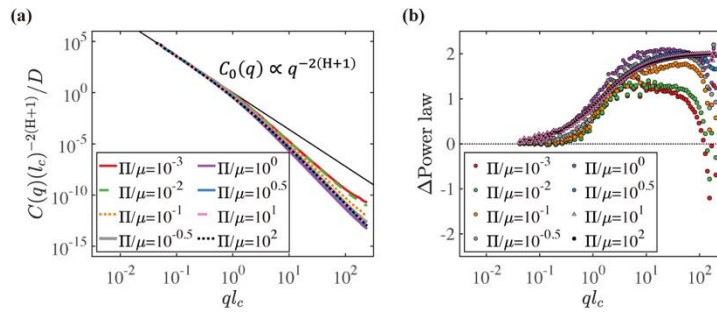


Figure S7. The effect Π/μ on the osmcapillary PSD prediction. (a) The dimensionless osmcapillary PSD. (b) Power law change between the osmcapillary PSD and the stress-free PSD.

Nondimensionalization of experimental PSD

To systematically compare the flattening effect on different samples, we need to first remove the effect of swelling relative to as-synthesized sample. As a reference, we first plot the PSD of all samples in the range $2 - 60 \mu\text{m}$ in Fig. S8a. Following the isotropic swelling assumption, we isotropically shrink the swollen surfaces. We shift the experimental PSD of each sample by $q(J/J_0)^{1/3}$ and $C(q)(J/J_0)^{-4/3}$ (Fig. S8b), then the effect of isotropic swelling is removed. Then we can nondimensionalize the PSD with $q(J/J_0)^{1/3}l_c$ and $\bar{C}(q) = C(q)(J/J_0)^{-4/3}(l_c)^{-2(1+H)}D^{-1}$ here $l_c = \max\{\gamma/\mu, \gamma/\Pi\}$ is the dominate capillary length.

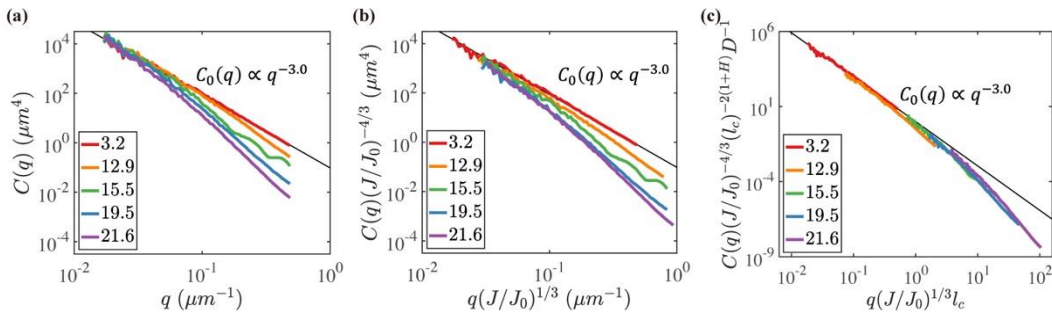


Figure S8. Nondimensionalization of experimental PSD. (a) Experimental PSD of all samples in the range $2 \mu\text{m} - 60 \mu\text{m}$. (b) Shifted experimental PSD of the as-synthesized and the swollen ionogels after removing the effect of isotropic swelling. (c) Shifted experimental PSD of the as-synthesized and the swollen ionogels after removing the effect of dominant capillary length.

References

1. M. Badv, I. H. Jaffer, J. I. Weitz and T. F. Didar, *Scientific reports*, 2017, **7**, 11639.
2. M. Larriba, S. García, J. Garcia, J. S. Torrecilla and F. Rodríguez, *Journal of Chemical & Engineering Data*, 2011, **56**, 3589-3597.
3. J. C. Day and I. D. Robb, *Polymer*, 1981, **22**, 1530-1533.
4. C. R. o. t. Web, Poly(acrylic acid), <http://polymerdatabase.com/polymers/polyacrylicacid.html>, (accessed May 22, 2023).
5. J. Zhu and Q. Liu, *Journal of the Mechanics and Physics of Solids*, 2023, **170**, 105124.